

Investigation of the filamin-A dependent mechanisms of tissue factor incorporation into microvesicles

Mary E W Collier^{1*}, Camille Ettelaie², Benjamin T Goult³, Anthony Maraveyas⁴, Alison H Goodall¹

¹Department of Cardiovascular Sciences, University of Leicester and NIHR Cardiovascular Biomedical Research Unit, Glenfield Hospital, Leicester, UK. ²Biomedical Section, School of Biological, Biomedical and Environmental Sciences, University of Hull, Hull, UK. ³School of Biosciences, University of Kent, Canterbury, Kent, UK. ⁴Division of Cancer, in association with Hull York Medical School, Hull, UK. ¹

*Correspondence to: Mary Collier, Department of Cardiovascular Sciences, University of Leicester and NIHR Cardiovascular Biomedical Research Unit, Glenfield Hospital, Leicester, LE3 9QP, UK.

Tel.: +44(0) 116 250 2650

E-mail: mec40@le.ac.uk

Short title: Collier. Mechanisms of TF incorporation into MVs

Text word count: 5079 words

Abstract word count: 249

Number of figures: 6

¹This work was supported by a grant from Yorkshire Cancer Research. Filamin-A cloning and *in vitro* binding assays were supported by an Eric Reid Methodology grant from the Biochemical Society.

Summary

We have previously shown that phosphorylation of tissue factor (TF) at Ser253 increases the incorporation of TF into microvesicles (MVs) following protease-activated receptor 2 (PAR2) activation through a process involving filamin-A, whereas Ser258 phosphorylation suppresses this process. Here we examined the contribution of the individual phosphorylation of these serine residues to the interaction between filamin-A and TF, and further examined how filamin-A regulates the incorporation of TF into MVs. *In vitro* binding assays using recombinant filamin-A C-terminal repeats 22-24 with biotinylated phospho-TF cytoplasmic domain peptides as bait, showed that filamin-A had the highest binding affinities for phospho-Ser253 and double-phosphorylated TF peptides, whilst the phospho-Ser258 TF peptide had the lowest affinity. Analysis of MDA-MB-231 cells using an *in situ* proximity ligation assay revealed increased proximity between the C-terminus of filamin-A and TF following PAR2 activation, which was concurrent with Ser253 phosphorylation and TF-positive MV release from these cells. Knock-down of filamin-A expression suppressed PAR2-mediated increases in cell surface TF procoagulant activity without reducing cell surface TF antigen expression. Disrupting lipid rafts by pre-incubation with methyl-beta cyclodextrin (M β CD) prior to PAR2 activation reduced TF-positive MV release and cell surface TF procoagulant activity to the same extent as filamin-A knock-down. In conclusion, this study shows that the interaction between TF and filamin-A is dependent on the differential phosphorylation of Ser253 and Ser258. Furthermore the interaction of TF with filamin-A may translocate cell surface TF to cholesterol-rich lipid rafts, increasing cell surface TF activity as well as TF incorporation and release into MVs.

Key words: Tissue factor, filamin-A, microvesicles, protease-activated receptor 2, lipid rafts

Tissue factor (TF) is a transmembrane protein that is expressed on the cell surface and released from cells in microvesicles (MVs). TF has a small cytoplasmic domain, which has no intrinsic kinase activity, and is not required for the procoagulant activity of TF [1]. However, serine residues 253 and 258 within the cytoplasmic domain of TF are phosphorylated following the activation of protein kinase C α (PKC α) [2] and p38 [3] respectively. The phosphorylation of Ser253 occurs first, which subsequently allows Ser258 to be phosphorylated [2]. TF phosphorylation mediates a number of cellular processes including cell migration [4], angiogenesis [5], VEGF production [6] and metastasis [7]. We have previously shown that the incorporation of TF into MVs following protease-activated receptor 2 (PAR2) activation is differentially regulated by the phosphorylation of Ser253 and Ser258, whereby phosphorylation of Ser253 promotes the incorporation of TF into MVs and phosphorylation of Ser258 suppresses this process [8]. We have also demonstrated that the presence of filamin-A is crucial for TF to be incorporated into MVs in response to PAR2 activation [9].

Filamin-A is a 280 kDa protein composed of an N-terminal actin-binding domain and 24 Ig-like repeats [10]. Repeat 24 allows filamin-A molecules to dimerise to form a “leaf spring” structure [10], while the actin binding domain cross-links actin filaments. Filamin-A also binds to over 90 transmembrane and cytosolic proteins [11], most of which interact with Ig repeats 16-24 of filamin-A, which regulates the function and cellular localisation of these proteins [11]. TF also binds to this region of filamin-A through a direct interaction between the cytoplasmic domain of TF and the C-terminus repeats 22-24 of filamin-A [12].

Furthermore, phosphorylation of the cytoplasmic domain of TF enhances the binding to filamin-A compared to non-phosphorylated TF [12]. However, the contribution of the individual phosphorylation at Ser253 and Ser258 to this interaction has not been explored.

The aim of this study was to determine whether the individual phosphorylation of TF at Ser253 and Ser258 differentially modulates the binding affinity of TF for filamin-A, in an attempt to further clarify the mechanism by which the sequential phosphorylation of Ser253 and Ser258 may regulate the incorporation of TF into MVs in a filamin-A dependent mechanism.

MATERIALS AND METHODS

Cloning and expression of repeats 22-24 of filamin-A

A synthetic gene encoding repeats 22-24 of filamin-A (amino acids 2329-2647) (GeneArt, Thermo Fisher Scientific, Paisley, UK) was sub-cloned into a bacterial expression vector in tandem with a N-terminal His ($\times 6$) tag by the Protein Expression Laboratory (University of Leicester, UK). The insert sequence was confirmed and the plasmid was transformed into *E.coli* BL21(DE3). Recombinant protein was isolated and purified on a nickel column using an AKTA purifier (GE Healthcare Life Sciences, Bucks, UK). The recombinant filamin-A was dialysed overnight in PBS and then examined by SDS-PAGE and western blot analysis to ensure it had the correct molecular weight (36 kDa) and was recognised by a filamin-A antibody (EP2405Y) (GeneTex Inc., CA, USA) directed against the 24th C-terminal repeat of filamin-A (Supplemental Figure 1).

TF cytoplasmic domain/recombinant filamin-A binding assays

High-binding 96-well plates (Greiner Bio-One Ltd, Gloucester, UK) were coated with 1 μ M of recombinant filamin-A repeats 22-24 or 1 μ M of BSA in 50 mM carbonate buffer, pH 9.6 overnight at 4°C. The plates were then washed three times with wash buffer (PBS, pH 7.4, 1 mM CaCl₂, 1 mM MgCl₂, 0.05 % (v/v) Tween-20) and blocked with 5 % (w/v) BSA in PBS for 1.5 h. The plates were washed three times and incubated for 2 h with 0-10 μ M of

biotinylated TF peptides corresponding to the final 19 amino acids of the cytoplasmic domain of TF (biotin-CRKAGVGQSWKENSPLNVS) with phosphorylation at Ser253 and/or Ser258 (shown as underlined), or non-phosphorylated (95 % purity) (Biomatik, Ontario, Canada).

The plates were washed three times and incubated for 1 h with streptavidin-HRP diluted 1:2000 (GE Healthcare Life Sciences). The plates were washed again and TMB One Solution (Promega, Southampton, UK) (100 µl) added and developed for 10 min. Reactions were stopped with 2 M sulphuric acid (50 µl) and the absorbance was recorded at 450 nm. Data were analysed using GraphPad Prism 6 using non-linear regression and one-site binding, and K_d values were calculated. The specific binding of TF peptides to recombinant filamin-A was calculated as the absorption values for the binding of the TF peptides to filamin-A following subtraction of the values for the binding of the TF peptides to BSA at each respective concentration of TF peptide.

Cell culture and transfection

The breast cancer cell line MDA-MB-231 was cultured in DMEM containing 10 % (v/v) heat-inactivated foetal calf serum (FCS) and maintained at 37°C under 5% (v/v) CO₂. Cells were seeded out into appropriate plates 48 h prior to experiments and adapted to serum-free medium (SFM) by 24 h incubation in 5 % (v/v) FCS medium, followed by two washes with PBS and 1 h incubation in SFM. Cells were then treated with PAR2-agonist peptide (PAR2-AP; SLIGKV-NH₂) (20 µM; Tocris Bioscience, Bristol, UK) or human factor VIIa (FVIIa) (5 nM; Enzyme Research Laboratories Ltd, Swansea, UK). In order to knock-down filamin-A expression, cells were reverse transfected with Silencer Select filamin-A siRNA (2 nM) or Silencer Select negative control siRNA1 (2 nM) using Lipofectamine RNAiMAX (all from Thermo Fisher Scientific) as previously described [10]. Primary endothelial cells (human dermal blood endothelial cells (HDBEC) (PromoCell, Heidelberg, Germany) and human

coronary artery endothelial cells (HCAEC) (PromoCell) were cultured at 37°C under 5% (v/v) CO₂ in endothelial cell growth medium MV (PromoCell) containing 5% (v/v) FCS and growth supplements (PromoCell). Endothelial cells were transfected with 1 µg of pCMV-XL5-TF in order to express wild-type TF (OriGene, Rockville, USA) or mutant forms of pCMV-XL5-TF with alanine or aspartate substitutions at serine residue 253 [8] using Lipofectin (Invitrogen, Paisley, UK). Following transfection, cells were incubated for 48 h at 37°C to allow TF expression.

Isolation and analysis of MVs from cell culture medium

MDA-MB-231 cells were cultured in T75 flasks until 80 % confluent, adapted to SFM as described previously and activated with PAR2-AP (20 µM) or FVIIa (5 nM) for 0-60 min. The culture medium was centrifuged at 1500 g for 15 min followed by centrifugation of the resultant supernatant at 40,000 g for 30 min at 20°C. The pelleted MVs were washed with HEPES buffered saline (HBS), pH 7.4 (10 ml) and centrifuged again. MVs were then resuspended in HBS (100 µl) and stored at -80°C.

The concentrations of MVs and the TF activity of the MVs were determined using the Calibrated Automated Thrombogram (CAT) assay. Platelet-poor pooled human plasma was prepared from blood from 15 healthy donors (ethical approval obtained from the University of Leicester) taken into 3.2 % (w/v) tri-sodium citrate, supplemented with corn trypsin inhibitor (CTI; Cambridge Biosciences) (18.3 µg/ml), and centrifuged at 1800 g for 30 min at room temperature. The plasma was aspirated and equal volumes from each donor pooled and then passed through 0.22 µm filters to remove endogenous MVs. The cell-derived MV samples were mixed with filtered pooled plasma at a ratio of 1:4. The MP reagent (4 µM phospholipids, no TF) (Diagnostica Stago Ltd, Ontario, Canada) was used to measure the TF activity of the MVs, and the PRP reagent (no phospholipids, 1 pM TF) was used to measure

the phospholipid-mediated procoagulant activity of the MV samples. MP or PRP reagent (20 μ l) was added to each well in 96-well plates followed by the addition of the MV/human plasma mix (80 μ l). Thrombin generation was then measured using the CAT assay on a Fluoroskan Ascent fluorimeter. Lag times and endogenous thrombin potential (ETP) were calculated using the Thrombinoscope software. MVs isolated from cells treated with FVIIa were measured using the Zymuphen MP activity assay (Hyphen-Bio Med, Neuville sur Oise, France) according to the manufacturers' instructions, due to interference from the added FVIIa in the CAT assay.

To measure the TF antigen content of the MVs by ELISA, MV samples were first supplemented with 1 % (v/v) Triton X-100 (to extract TF out of MVs) and then diluted 1:1 in diluent buffer and quantified using the Tissue Factor Quantikine ELISA kit (R&D Systems, Abingdon, UK) according to the manufacturer's instructions.

Immunoprecipitation of TF

MDA-MB-231 cells were cultured to 80 % confluence in T25 flasks, adapted to SFM as described previously and activated with PAR2-AP (20 μ M) or FVIIa (5 nM). Cells were washed with PBS and lysed in Phospho-Safe lysis buffer (Merck-Millipore, Nottingham, UK) (500 μ l) containing protease inhibitor cocktail (1% v/v) (P8340; Sigma Chemical Company Ltd, Poole, UK). The lysates were centrifuged at 10,000 *g* on a microcentrifuge for 10 min and the supernatant incubated with the mouse anti-TF antibody HTF1 (10 μ g; Affymetrix eBioscience, Altrincham, UK) or mouse control IgG (Cell Signalling Technology) at 4°C overnight. PureProteome protein A-magnetic beads (15 μ l; Merck-Millipore) were added to the samples and incubated at 4°C for 90 min. The beads were then washed five times with PBS, pH 7.2 (1 ml) containing 0.05% (v/v) Tween-20 and denatured by boiling in Laemmli's buffer (70 μ l; Sigma) for 10 min. The supernatant was removed from the beads and proteins

were separated by 12 % (w/v) SDS-PAGE. Membranes were probed with a rabbit anti-TF antibody (FL-295; Santa Cruz Biotechnology Inc., Heidelberg, Germany), a rabbit anti-phospho-serine PKC substrate antibody (New England Biolabs), or a rabbit anti-phospho-Ser258 TF antibody (Abcam, Cambridge, UK) and detected using an anti-rabbit alkaline phosphatase-conjugated secondary antibody (Santa Cruz Biotechnology). The membranes were developed with Western Blue substrate for alkaline phosphatase (Promega). Images were acquired on an ImageQuant LAS-4000 imager (GE Healthcare) and densitometry was carried out using the ImageQuant software.

Duolink proximity ligation assays (PLA)

MDA-MB-231 cells (10^4) were seeded out into 96-well plates (Greiner Bio One), adapted to SFM as described previously and incubated with PAR2-AP (20 μ M) or FVIIa (5 nM). The cells were fixed for 15 min with 4% (v/v) paraformaldehyde, washed three times with PBS, permeabilised with saponin (0.2% (v/v)) for 5 min and blocked with Duolink blocking buffer (Sigma) for 1 h. Samples were incubated overnight at 4°C with the mouse anti-TF antibody HTF1 (5 μ g/ml) together with the rabbit anti-filamin-A antibody EP2405Y (raised against the C-terminus of filamin-A) (2.6 μ g/ml) in Tris-buffered saline (TBS) (20 mM Tris-HCl, pH7.4, 150 mM NaCl) supplemented with 1 % (v/v) blocking buffer. The anti-filamin-A antibody was replaced with rabbit IgG (New England Biolabs) (2.6 μ g/ml), or the anti-TF antibody was replaced with normal mouse IgG (5 μ g/ml) in negative control samples. The cells were washed three times with TBS containing 0.05% (v/v) Tween-20 (TBST) and the PLA procedure carried out according to the manufacturer's instructions. The actin cytoskeleton was labelled by incubation with Acti-stain 488 (100 nM) (Cytoskeleton Inc., Denver, USA) and nuclei were labelled with DAPI (2 μ g/ml) (Sigma). Images were acquired using an

EVOS fluorescent microscope (Thermo Fisher Scientific). The number of red fluorescent events and nuclei were determined using ImageJ.

Flow cytometry for cell surface TF

MDA-MB-231 cells (2×10^5) were seeded out into 6-well plates, adapted to SFM as described previously and incubated with PAR2-AP (20 μ M) or FVIIa (5 nM) for 30 min. Cells were then detached using TrypLE Select (Thermo Fisher Scientific), pelleted by centrifugation at 260 g for 5 min on a microcentrifuge and washed with HBS containing 0.1% (w/v) bovine serum albumin (BSA) and 0.1% (v/v) sodium azide. Cells were incubated for 60 min on ice in HBS/BSA/sodium azide containing either the mouse anti-TF Alexa Fluor-488 antibody (R&D Systems) or mouse IgG Alexa Fluor-488 isotype control antibody (R&D Systems) at a final concentration of 1 μ g/ml. Cells were analysed using a CyAn flow cytometer (Beckman Coulter) with a gate set at 2 % of the control IgG. Data were analysed using the Summit software (Beckman Coulter).

Cell surface TF activity assay

MDA-MB-231 cells (5×10^3) were seeded out into 96-well plates, adapted to SFM as described previously and incubated with PAR2-AP (20 μ M) for 30 min. Cells were then washed twice with HBS containing 1 mg/ml BSA and 0.1 % (v/v) sodium azide (200 μ l), and incubated with either the mouse anti-TF inhibitory antibody HTF1 (40 μ g/ml) to block TF procoagulant activity, or mouse control IgG antibody (40 μ g/ml) at room temperature for 15 min. Filtered platelet-poor pooled human plasma containing CTI (18.3 μ g/ml) (60 μ l) was then added to each well and thrombin generation was measured using the CAT assay in the absence of any exogenous reagent. TF-specific thrombin generation was calculated as the

ETP of samples incubated with control IgG minus the ETP of samples incubated with the inhibitory TF antibody HTF1.

Statistical analysis

Data represent the calculated mean values from the number of experiments stated in the figure legends \pm the calculated standard error of the mean (SEM). The data were analysed using the statistical package for the social sciences (SPSS). Significance was determined using one-way ANOVA and the Tukey's honestly significance test and values of $p < 0.05$ were considered to be significant.

RESULTS

Phosphorylation of serine residues 253 and 258 within the cytoplasmic domain of TF alters the interaction with filamin-A

Initially, the binding of peptides corresponding to the final 19 amino acids of the cytoplasmic domain of TF to recombinant repeats 22-24 of filamin-A was examined using an *in vitro* binding assay. The phospho-Ser253 TF peptide and the double phosphorylated peptide had the greatest binding affinities for the C-terminal repeats 22-24 of filamin-A (Figure 1A), with K_d values of $2.35 \pm 0.37 \mu\text{M}$ and $2.61 \pm 0.84 \mu\text{M}$ ($n=8$) respectively. Conversely, the phospho-Ser258 TF peptide exhibited the lowest affinity for filamin-A ($K_d = 7.34 \pm 0.79 \mu\text{M}$), with the non-phosphorylated TF peptide having an intermediate affinity ($K_d = 3.63 \pm 0.93 \mu\text{M}$) ($n=8$). To confirm these data, non-biotinylated phospho-Ser253 and non-biotinylated double phosphorylated TF peptides were used to compete out binding of biotinylated TF peptides in different phosphorylation states. In the presence of the highest concentration of the non-biotinylated phospho-Ser253 peptide, the binding of the phospho-Ser258 peptide was reduced

by up to 68.5 ± 12.7 %, and the non-phosphorylated TF peptide was competed out by 19 ± 11.4 %, however there was no significant influence on the binding of the double phosphorylated TF peptide (Figure 1B). Similar results were observed with increasing concentrations of the non-biotinylated phospho-Ser253/258 peptide to compete out binding of the biotinylated phospho-Ser258 peptide to recombinant filamin-A (Figure 1C). A polyclonal anti-filamin-A antibody also competed out the binding of the phospho-Ser253 TF peptide, indicating that the binding was mediated through repeats 22-24 of filamin-A (Figure 1D).

Activation of PAR2 results in TF phosphorylation and increased release of TF-positive MVs

Following the activation of MDA-MB-231 cells with PAR2-AP (20 μ M) (Figure 2A) or FVIIa (5 nM) (Supplemental Figure 2A) a trend was observed for cells to release increased levels of phosphatidylserine-positive MVs over 60 min, which was accompanied by higher MV-associated TF antigen levels (Figure 2B). MVs released in response to PAR2-AP also had significantly increased TF activity as shown by a decrease in lag time in the CAT assay (n=3; p=0.233 60 min incubation with PAR2-AP vs. untreated control) (Supplemental Figure 2B). The procoagulant activity associated with the MVs was TF-dependent because pre-incubation of the samples with the inhibitory TF antibody HTF1 reduced the endogenous thrombin potential and extended the lag time to >25 min (Supplemental Figure 3). Incubation of MDA-MB-231 cells with PAR2-AP also resulted in a significant increase in the phosphorylation of TF at Ser253, with maximal levels observed at 30 min activation (Figures 2C&E). Ser253 phosphorylation was followed by phosphorylation of Ser258 which peaked at 50 min post-activation with PAR2-AP (Figures 2D&E). Data from two experiments showed a similar pattern of TF phosphorylation in cells activated with FVIIa (Supplemental Figure 4).

The release of TF-positive MVs and the phosphorylation of TF at serine residues 253 and 258 in endothelial cells following PAR2 activation has been shown previously [8].

Activation of PAR2 results in increased proximity of TF and filamin-A in MDA-MB-231 cells and primary endothelial cells

The proximity of TF and filamin-A was examined by an *in situ* procedure employing the Duolink proximity ligation assay, which permits the detection of two molecules within close (≤ 40 nm) proximity of each other [13]. Close proximity between TF and the C-terminus of filamin-A was detectable in non-activated MDA-MB-231 cells, and a trend was observed for the number of interactions per cell to increase following PAR2 activation with the agonist peptide, reaching the maximum at 40 min (Figure 3A & Supplemental Figure 5A). Furthermore, treatment of cells with FVIIa resulted in a significant increase in interactions between TF and filamin-A ($n=3$, $p=0.027$ vs. untreated cells) (Supplemental Figure 5B). In contrast, few TF-filamin-A interactions were detected in non-activated primary endothelial cells transfected to express low levels of TF (Supplemental Figure 5C). However, as with MDA-MB-231 cells there was a trend for the number of interactions to increase in both types of endothelial cells following PAR2 activation (Supplemental Figure 5C). Fewer TF-filamin-A interactions were detected in endothelial cells compared to MDA-MB-231 cells, with only a few events observed per cell, probably as a result of low levels of TF expression. Co-immunoprecipitation of TF and filamin-A using either anti-TF or anti-filamin-A antibodies was not possible, and pull-down assays using the TF cytoplasmic domain peptides conjugated to magnetic beads did not pull-down filamin-A from cell lysates.

Phosphorylation of serine residue 253 within the TF cytoplasmic domain enhances the proximity of TF and filamin-A in endothelial cells

In order to examine whether serine 253 phosphorylation enhances the interaction between TF and filamin-A in cells, primary endothelial cells (HDBEC) were transfected to express mutant forms of TF with substitution of serine 253 with an alanine residue (to prevent phosphorylation) or an aspartate residue (to mimic phospho-serine) and analysed by PLA. Transfected endothelial cells expressed similar levels of wild-type and mutant forms of TF (Supplemental Figure 6). Alanine-substitution of residue 253 resulted in lower proximity between TF and filamin-A in PAR2-activated cells compared to activated cells expressing wild-type TF (Figure 3B). In contrast, increased proximity between TF and filamin-A was observed in cells expressing the aspartate 253-substituted TF above levels observed in cells expressing wild-type TF, in both non-activated and PAR2-activated cells (Figure 3B).

Knock-down of filamin-A expression prevents PAR2-mediated increases in cell surface TF activity on MDA-MB-231 cells

We have previously shown that knock-down of filamin-A expression suppresses the incorporation of TF into MVs in response to PAR2 activation [9], although the underlying mechanism is unclear. Therefore, here we examined whether filamin-A regulates the translocation of TF to the cell surface, or alternatively if it controls the cell surface localisation of TF, facilitating the incorporation of TF into MVs. As shown previously [9], reverse-transfection of MDA-MB-231 cells with 2 nM of filamin-A Silencer Select siRNA resulted in the partial knock-down of filamin-A expression, but did not alter TF expression (Supplemental Figure 7). Suppression of filamin-A expression using specific siRNA abolished increases in TF-specific thrombin generation following PAR2 activation in transfected MDA-MB-231 cells compared to that observed on the surface of MDA-MB-231

cells transfected with control siRNA (Figure 4A). The increase in thrombin generation was shown to be predominantly TF-specific and was suppressed by incubation of the cells with the inhibitory TF antibody HTF1 (40 µg/ml) (Supplemental Figure 8). In contrast, filamin-A knock-down increased levels of TF antigen on the surface of MDA-MB-231 cells compared to cells transfected with control siRNA (Figures 4B&C). A similar trend was observed in levels of cell surface TF antigen in filamin-A siRNA-transfected cells compared to non-transfected cells, indicating that transfection with siRNA itself had no effect on overall cellular behaviour (Supplemental Figure 9).

Disruption of lipid rafts reduces TF-MV release and suppresses PAR2-mediated increases in cell surface TF activity

A recent study has shown that macrophage-derived TF-positive MVs originate from lipid rafts [14]. Furthermore, TF associated with cholesterol-rich microdomains has been shown to possess increased procoagulant activity [15]. Therefore, since filamin-A knock-down suppressed PAR2-mediated increases in cell surface TF activity (Figure 4A), we tested whether filamin-A is required for the translocation of TF into cholesterol-rich microdomains and subsequent incorporation into MVs. Depletion of membrane cholesterol from MDA-MB-231 cells with methyl beta cyclodextrin (MβCD) significantly reduced the release of MVs from MDA-MB-231 cells (Figure 5A). Similarly, treatment of cells with MβCD also reduced the associated TF activity of these MVs (Figure 5B). Consequently, the outcome of concurrent filamin-A knock-down and lipid raft disruption on TF activity on the surface of cells was examined. Cell surface TF activity was reduced in the presence of MβCD alone (Figure 5C), in agreement with previous reports that lipid rafts support TF procoagulant activity [15, 16]. Both pre-incubation of the cells with MβCD or the suppression of filamin-A expression reduced cell surface TF activity to similar levels following PAR2 activation. In

addition, no additional or co-operative reduction in TF activity was observed on pre-incubation of filamin-A knock-down cells with M β CD (Figure 5C). To examine whether TF phosphorylation alone is sufficient for TF to be translocated to lipid rafts and therefore increase TF procoagulant activity, MDA-MB-231 cells were incubated with PMA (100 nM) for 30 min to directly activate PKC α and induce TF phosphorylation [17]. Analysis of PMA-treated and untreated cells showed no differences in levels of cell surface TF activity, which was also unaltered by suppression of filamin-A expression (Supplemental Figure 10). Increased levels of phosphatidylserine (PS) on the outer leaflet of the plasma membrane can also augment TF procoagulant activity [18]. Therefore the effect of the suppression of filamin-A expression on levels of cell surface PS was examined by flow cytometry for annexin V binding, and showed that cells with filamin-A knock-down had marginally higher levels of cell surface PS compared to cells transfected with control siRNA (Figure 6).

DISCUSSION

We previously reported that the incorporation of TF into MVs in response to PAR2 activation is promoted by the phosphorylation of TF at Ser253, and subsequently suppressed by phosphorylation of Ser258 [8]. Furthermore, we have shown that filamin-A is essential for the increased incorporation of TF into MVs following PAR2 activation [9]. However, the underlying mechanisms of filamin-A-dependent incorporation of TF into MVs are not known. Since filamin-A binds to the cytoplasmic domain of TF in a phosphorylation-dependent manner [12] the main aim of this study was to examine the individual role of Ser253 and Ser258 in the interaction between filamin-A and TF. *In vitro* binding assays revealed that both the phospho-Ser253 TF peptide and dual phosphorylated TF peptide had the highest binding affinities for the C-terminus repeats 22-24 of filamin-A (Figure 1A). In contrast, the phospho-Ser258 TF peptide showed a low binding affinity for repeats 22-24 of

filamin-A, even below that of the non-phosphorylated TF peptide. This indicates that the phosphorylation of Ser253 is essential for the interaction with repeats 22-24 of filamin-A, and that additional phosphorylation of Ser258 does not interfere with this process *per se*.

However, phosphorylation of Ser258 and the subsequent de-phosphorylation of Ser253 acts as a molecular switch, and therefore the two phosphorylation sites have opposing roles in regulating the binding of TF to the C-terminus of filamin-A. Since filamin-A is essential for the incorporation of TF into MVs this may also explain the contrasting effects of Ser253 and Ser258 phosphorylation on TF incorporation into MVs [8].

Because the values for the binding affinities of the TF cytoplasmic domain peptides to filamin-A were in the μM range, this low binding affinity and transient nature of the interaction may explain why co-immunoprecipitation of TF and filamin-A was not possible. Therefore, proximity ligation assays were employed to detect TF: filamin-A interactions *in situ*. We used MDA-MB-231 cells throughout the study as they release TF in a filamin-A dependent manner in response to PAR2 activation (Figures 2A&B) [9]. Increased proximity between TF and filamin-A following PAR2 activation was shown to be transient in both MDA-MB-231 cells (Figure 3) and endothelial cells (Supplemental Figure 5C). The direct interaction of the C-terminus of filamin-A with the cytoplasmic domain of TF phosphorylated at both Ser253 and Ser258 has been demonstrated previously [12]. Also, TF has been shown to co-localise with filamin-A at the leading edge of spreading epithelial cells [19] and in migrating smooth muscle cells [20]. However, this is the first study to demonstrate the opposing roles of the individual phosphorylation of TF at Ser253 and Ser258 on its interaction with filamin-A. The dissimilar binding affinities between filamin-A and TF in different phosphorylation states may arise due to structural changes within the cytoplasmic domain of TF which occur following phosphorylation of Ser253 and Ser258 [21], and/or changes in the structure of filamin-A following cellular activation [22, 23]. Further

investigation of the structure of filamin-A in complex with the phospho-TF peptides would be required to determine the conformation of filamin-A with TF in different phosphorylation states.

Since MVs are derived from the cell surface and incorporate cell surface antigens, the role of filamin-A in localising TF to the cell surface or to specific membrane microdomains for incorporation into MVs was examined. Here we report for the first time that filamin-A is required for the increased cell surface TF activity in response to PAR2 activation in these cells, since knock-down of filamin-A suppressed this process (Figure 4A). In contrast, cell surface TF antigen increased in cells with suppression of filamin-A expression, possibly because TF could not be incorporated into MVs and therefore accumulated on the cell surface. Filamin-A links receptors to the actin cytoskeleton to stabilise receptors at the cell surface [24, 25] and regulate receptor internalisation [26, 27]. It is possible that filamin-A links TF to the actin cytoskeleton to translocate TF to sites of MV release. Furthermore, the interaction between filamin-A and TF is unlikely to have a role in the transport of TF from intracellular stores to the cell surface [28], since suppression of filamin-A expression resulted in increased levels of cell surface TF antigen. This is in agreement with an observation by Rothmeier *et al.* (2015) that cell surface TF, rather than TF transported from the Golgi, is incorporated into macrophage-derived MVs [14].

It has been reported that TF-positive MVs are derived from lipid rafts [14, 29, 30, 31]. In agreement with this we found that cholesterol depletion reduced TF-positive MV release (Figures 5A&B). Furthermore, disruption of lipid rafts using M β CD reduced cell surface TF-specific procoagulant activity (Figure 5C). This is in agreement with previous studies that have shown that cholesterol depletion using M β CD reduces TF procoagulant activity by

lowering the binding affinity of cell surface TF for FVIIa [15, 16]. Importantly, cell surface PS levels were not reduced by knock-down of filamin-A expression (Figure 6), discounting the reduced exposure of PS on the cell surface as the reason for the observed reduction in cell surface TF procoagulant activity on cells with suppression of filamin-A expression.

Furthermore, M β CD did not alter the effect of filamin-A knock-down on TF cell surface activity following PAR2 activation. In fact M β CD had a similar effect as filamin-A knockdown, but there was no additive or co-operative reduction in TF activity (Figure 5C). This indicates that both filamin-A knock-down and treatment with M β CD work through a similar mechanism, interfering with the association of TF with cholesterol-rich microdomains necessary for optimal TF activity. Therefore, the interaction with filamin-A is likely to be required for the translocation of cell surface TF following PAR2 activation to cholesterol rich microdomains, that subsequently allows incorporation of active TF into MVs. This is compatible with the concept that transmembrane proteins can translocate to lipid rafts following cellular activation [32, 33], and filamin-A has been shown to cluster and retain receptors at the cell surface [24, 25, 34]. TF is known to be associated within distinct fractions following membrane fractionation by sucrose density gradient ultracentrifugation [16]. Therefore, in future experiments we aim to examine the lipid raft distribution of cell surface TF following suppression of filamin-A expression.

In conclusion, this study has for the first time demonstrated the opposing roles of Ser253 and Ser258 phosphorylation in the interaction between TF and filamin-A. Furthermore, the data suggest the filamin-A dependent translocation of TF into lipid-rich microdomains as the mechanism by which filamin-A mediates the incorporation and release of TF into MVs following PAR2 activation.

ACKNOWLEDGMENTS

We thank Dr Kees Straatman for developing the ImageJ macro to analyse the PLA images.

REFERENCES

1. Mueller BM, Ruf W. Requirement for binding of catalytically active factor VIIa in tissue factor-dependent experimental metastasis. *J Clin Invest* 1998; 10: 1372-1378.
2. Ahamed J, Ruf W. Protease-activated receptor 2-dependent phosphorylation of the tissue factor cytoplasmic domain. *J Biol Chem* 2004; 279: 23038-23044.
3. Ettelaie C, Elkeeb AM, Maraveyas A, et al. p38 α phosphorylates serine 258 within the cytoplasmic domain of tissue factor and prevents its incorporation into cell-derived microparticles. *Biochim Biophys Acta* 2013; 1833: 613-621.
4. Siegbahn A, Johnell M, Sorensen BB, et al. Regulation of chemotaxis by the cytoplasmic domain of tissue factor. *Thromb Haemost* 2005; 93: 27-34.
5. Belting M, Dorrell MI, Sandgren S, et al. Regulation of angiogenesis by tissue factor cytoplasmic domain signaling. *Nat Med* 2004; 10: 502-509.
6. Abe K, Shoji M, Chen J, et al. Regulation of vascular endothelial growth factor production and angiogenesis by the cytoplasmic tail of tissue factor. *Proc Natl Acad Sci U S A* 1999; 96: 8663-8668.
7. Bromberg ME, Sundaram R, Homer RJ, et al. Role of tissue factor in metastasis: functions of the cytoplasmic and extracellular domains of the molecule. *Thromb Haemost* 1999; 82: 88-92.

8. Collier ME, Ettelaie C. Regulation of the incorporation of tissue factor into microparticles by serine phosphorylation of the cytoplasmic domain of tissue factor. *J Biol Chem* 2011; 286: 11977-11984.
9. Collier ME, Maraveyas A, Ettelaie C. Filamin-A is required for the incorporation of tissue factor into cell-derived microvesicles. *Thromb Haemost* 2014; 111: 647-655.
10. Gorlin JB, Yamin R, Egan S, et al. Human endothelial actin-binding protein (ABP-280, nonmuscle filamin): a molecular leaf spring. *J Cell Biol* 1990; 111: 1089-1105.
11. Nakamura F, Stossel TP, Hartwig JH. The filamins: organizers of cell structure and function. *Cell Adh Migr* 2011; 5: 160-169.
12. Ott I, Fischer EG, Miyagi Y, et al. A role for tissue factor in cell adhesion and migration mediated by interaction with actin-binding protein 280. *J Cell Biol* 1998; 140: 1241-1253.
13. Koos B, Andersson L, Clausson CM, et al. Analysis of protein interactions in situ by proximity ligation assays. *Curr Top Microbiol Immunol* 2014; 377: 111-126.
14. Rothmeier AS, Marchese P, Petrich BG, et al. Caspase-1-mediated pathway promotes generation of thromboinflammatory microparticles. *J Clin Invest* 2015; 125: 1471-1484.
15. Mandal SK, Iakhiaev A, Pendurthi UR, et al. Acute cholesterol depletion impairs functional expression of tissue factor in fibroblasts: modulation of tissue factor activity by membrane cholesterol. *Blood* 2005; 105: 153-160.
16. Awasthi V, Mandal SK, Papanna V, et al. Modulation of tissue factor-factor VIIa signaling by lipid rafts and caveolae. *Arterioscler Thromb Vasc Biol* 2007; 27: 1447-1455.
17. Zioncheck TF, Roy S, Vehar GA. The cytoplasmic domain of tissue factor is phosphorylated by a protein kinase C-dependent mechanism. *J Biol Chem* 1992; 267: 3561-3564.

18. Bach R, Rifkin DB. Expression of tissue factor procoagulant activity: regulation by cytosolic calcium. *Proc Natl Acad Sci U S A* 1990; 87: 6995-6999.
19. Müller M, Albrecht S, Gölfert F, et al. Localization of tissue factor in actin-filament-rich membrane areas of epithelial cells. *Exp Cell Res* 1999; 248: 136-147.
20. Peña E, Arderiu G, Badimon L. Subcellular localization of tissue factor and human coronary artery smooth muscle cell migration. *J Thromb Haemost* 2012; 10: 2373-2382.
21. Sen M, Herzik M, Craft JW, et al. Spectroscopic Characterization of Successive Phosphorylation of the Tissue Factor Cytoplasmic Region. *Open Spectrosc J* 2009; 3: 58-64.
22. Ruskamo S, Gilbert R, Hofmann G, et al. The C-terminal rod 2 fragment of filamin A forms a compact structure that can be extended. *Biochem J* 2012; 446: 261-269.
23. Chen H, Zhu X, Cong P, et al. Differential mechanical stability of filamin A rod segments. *Biophys J* 2011; 101: 1231-1237.
24. Smith L, Page RC, Xu Z, et al. Biochemical basis of the interaction between cystic fibrosis transmembrane conductance regulator and immunoglobulin-like repeats of filamin. *J Biol Chem* 2010; 285: 17166-17176.
25. Lin R, Karpa K, Kabbani N, et al. Dopamine D2 and D3 receptors are linked to the actin cytoskeleton via interaction with filamin A. *Proc Natl Acad Sci U S A* 2001; 98: 5258-5263.
26. Seck T, Baron R, Horne WC. Binding of filamin to the C-terminal tail of the calcitonin receptor controls recycling. *J Biol Chem* 2003; 278: 10408-10416.
27. Zhang M, Breitwieser GE. High affinity interaction with filamin A protects against calcium-sensing receptor degradation. *J Biol Chem* 200; 280: 11140-11146.
28. Kanaji T, Ware J, Okamura T, et al. GPIIb α regulates platelet size by controlling the subcellular localization of filamin. *Blood* 2012; 119: 2906-2913.

29. Del Conde I, Shrimpton CN, Thiagarajan P, et al. Tissue-factor-bearing microvesicles arise from lipid rafts and fuse with activated platelets to initiate coagulation. *Blood* 2005; 106: 1604-1611.
30. Burger D, Montezano AC, Nishigaki N, et al. Endothelial microparticle formation by angiotensin II is mediated via Ang II receptor type I/NADPH oxidase/ Rho kinase pathways targeted to lipid rafts. *Arterioscler Thromb Vasc Biol* 2011; 31: 1898-1907.
31. Biró E, Akkerman JW, Hoek FJ, et al. The phospholipid composition and cholesterol content of platelet-derived microparticles: a comparison with platelet membrane fractions. *J Thromb Haemost* 2005; 3: 2754-2763.
32. Petrie RJ, Schnetkamp PP, Patel KD, et al. Transient translocation of the B cell receptor and Src homology 2 domain-containing inositol phosphatase to lipid rafts: evidence toward a role in calcium regulation. *J Immunol* 2000; 165: 1220-1227.
33. Lacour S, Hammann A, Grazide S, et al. Cisplatin-induced CD95 redistribution into membrane lipid rafts of HT29 human colon cancer cells. *Cancer Res* 2004; 64: 3593-3598.
34. Thelin WR, Chen Y, Gentzsch M, et al. Direct interaction with filamins modulates the stability and plasma membrane expression of CFTR. *J Clin Invest* 2007; 117: 364-374.

Disclosures: None.

FIGURE LEGENDS

Figure 1. TF peptide: recombinant filamin-A *in vitro* binding assays. A) Biotinylated TF peptides in non-phosphorylated, Ser253 or Ser258 phosphorylated, or double phosphorylated forms were incubated in plates coated with recombinant filamin-A repeats 22-24 (1 μ M) or BSA for 2 h. Unbound peptides were removed by washing, and bound TF peptides were detected using streptavidin-HRP and TMB substrate (n=8, * = $p < 0.0001$ vs. non-phosphorylated peptide, ** = $p < 0.002$ vs. non-phosphorylated peptide). B) Increasing concentrations of the unlabelled phospho-Ser253 TF peptide (0.1-10 μ M) were used to compete out the binding of biotinylated TF peptides (10 μ M) in non-phosphorylated, phospho-Ser258 and double phosphorylated forms to recombinant filamin-A. Data show the percentage change in binding for each peptide compared to binding in the absence of unlabelled phospho-Ser253 TF peptide (n =8, * = $p < 0.037$ vs. double phosphorylated TF peptide in the presence of 1 μ M of unlabelled phospho-S253 peptide, ** = $p < 0.0001$ vs. non-phosphorylated and double phosphorylated peptides in the presence of 5 and 10 μ M of unlabelled phospho-Ser253 peptide). C) Increasing concentrations of the unlabelled phospho-Ser253/258 TF peptide (0.1-10 μ M) were used to compete out the binding of biotinylated TF peptides (10 μ M) in non-phosphorylated, phospho-Ser253 and phospho-Ser258 forms to recombinant filamin-A. Data show the percentage change in binding for each peptide compared to binding in the absence of the unlabelled phospho-S253/258 TF peptide (n =8, * = $p < 0.013$ vs. non-phosphorylated TF peptide in the presence of 1 μ M of unlabelled phospho-Ser253/258 peptide, ** = $p < 0.001$ vs. non-phosphorylated peptide in the presence of 5 μ M of unlabelled phospho-Ser253/258 TF peptide, *** = $p < 0.0001$ vs. non-phosphorylated peptide and phospho-Ser253 peptide in the presence of 10 μ M of unlabelled phospho-Ser253/258 TF peptide). D) Biotinylated phospho-Ser253 TF peptide (10 μ M) was incubated in recombinant filamin-A-coated plates in the presence of increasing

concentrations of an anti-filamin-A polyclonal antibody (n=8, * = p <0.017 vs. sample without antibody).

Figure 2. TF-MV release and TF phosphorylation in MDA-MB-231 cells following PAR2 activation

MDA-MB-231 cells were activated with PAR2-AP (20 μ M) and MVs were isolated at intervals over 60 min. A) The concentrations of the isolated MVs were measured using the CAT assay with the PRP reagent (n=3) and B) the TF content of the isolated MVs was determined using the TF-ELISA (n=3). C, D, E) MDA-MB-231 cells were activated with PAR2-AP (20 μ M) for 0-60 min and TF was immunoprecipitated using the anti-TF antibody HTF1. The phosphorylation of C) Ser253 and D) Ser258 was examined by SDS-PAGE and western blot analysis (n=5, * = p 0.035 vs. 0 min). E) Western blot images for total TF (FL-295), phospho-Ser253 (phospho-serine PKC site antibody) and phospho-Ser258.

Figure 3. Increased proximity of filamin-A and TF in MDA-MB-231 cells and primary endothelial cells following PAR2 activation

A) MDA-MB-231 cells were activated with PAR2-AP (SLIGKV, 20 μ M) for 0-60 min, fixed and then incubated with anti-TF antibody (HTF1) together with the anti-filamin-A antibody EP2405Y. In control reactions, HTF1 and EP2405Y were replaced with mouse or rabbit IgG respectively. The proximity ligation assays were carried out using the DuoLink assay. Nuclei were stained with DAPI and the actin cytoskeleton was stained using Acti-stain phalloidin-488 (n=4). B) HDBEC were transfected to express wild-type TF (WT), or TF with alanine (Ala253) or aspartate (Asp253) substitutions of serine 253. Cells were activated with PAR2-AP (20 μ M) for 45 min and the proximity of TF and filamin-A was examined using the PLA

procedure. IgG = TF antibody replaced with mouse control IgG. (n=4, * = p<0.05 vs. WT without PAR2 activation. ** = p<0.01 vs. WT with PAR2-AP, # = p<0.0001 vs. Asp253 with PAR2 activation).

Figure 4. Filamin-A knock-down suppresses PAR2-mediated increase in cell surface TF activity

A-C) MDA-MB-231 cells were transfected with filamin-A siRNA or control siRNA (2 nM). Following 48 h incubation the cells were activated with PAR2-AP (SLIGKV) for 30 min. A) Cells were then incubated with either the TF inhibitory antibody HTF1 or control IgG (40 µg/ml) for 15 min and cell surface TF-specific thrombin generation was determined using the CAT assay in the absence of the any exogenous reagent (n=5, * = p <0.05 vs. untreated cells with control siRNA, ** = p< 0.002 vs. SLIGKV treated cells with control siRNA). B&C) Cell surface TF on MDA-MB-231 cells with knock-down of filamin-A expression following PAR2 activation was examined by flow cytometry and B) the mean fluorescence intensity and C) percentage of positive cells were measured (n=3, * = p 0.0001 vs. respective siRNA control).

Figure 5. Disrupting cholesterol-rich microdomains prevents PAR2-mediated increases in cell surface TF activity.

MDA-MB-231 cells were reverse transfected with filamin-A siRNA or control siRNA (2 nM). Following 48 h incubation the cells were incubated with MβCD (7.5 mM) and PAR2-AP (SLIGKV, 20 µM) for 30 min. TF-MV release was examined by measuring A) PS-positive MV release using the CAT assay with the PRP reagent (n=5, * = p 0.009 vs. SLIGKV, ** = p 0.029 vs. untreated control) and B) TF activity of the MVs using the CAT

assay with the MP reagent (n=5, * = p 0.04 vs. untreated control). C) Cells were incubated with either the anti-TF inhibitory antibody HTF1 or control IgG (40 µg/ml) for 15 min and cell surface TF-specific thrombin generation on cells with knock-down of filamin-A expression was determined using the CAT assay in the absence of any exogenous reagent (n=5, * = p <0.05 vs. untreated cells with control siRNA, ** = p< 0.002 SLIGKV vs. SLIGKV treated cells with control siRNA, *** = p<0.0001 MβCD vs. SLIGKV treated cells with control siRNA).

Figure 6. Filamin-A knock-down does not reduce cell surface phosphatidylserine

MDA-MB-231 cells were reverse transfected with filamin-A or control siRNA (2 nM). Following 48 h incubation the cells were adapted to serum-free medium and activated with PAR2-AP (SLIGKV, 20 µM) for 30 min. Cells were detached using TrypLE Select, washed and then resuspended in HBS, pH 7.4 containing calcium chloride (2 mM). Negative controls were incubated with HBS lacking calcium chloride. Cells were incubated with 5 µl of annexin V-FITC (BD Biosciences) for 20 min on ice. The cells were then examined by flow cytometry using a Gallios flow cytometer. A gate was set at 2 % of cells incubated with annexin V-FITC in the absence of calcium chloride (n = 4).

Figure 1.

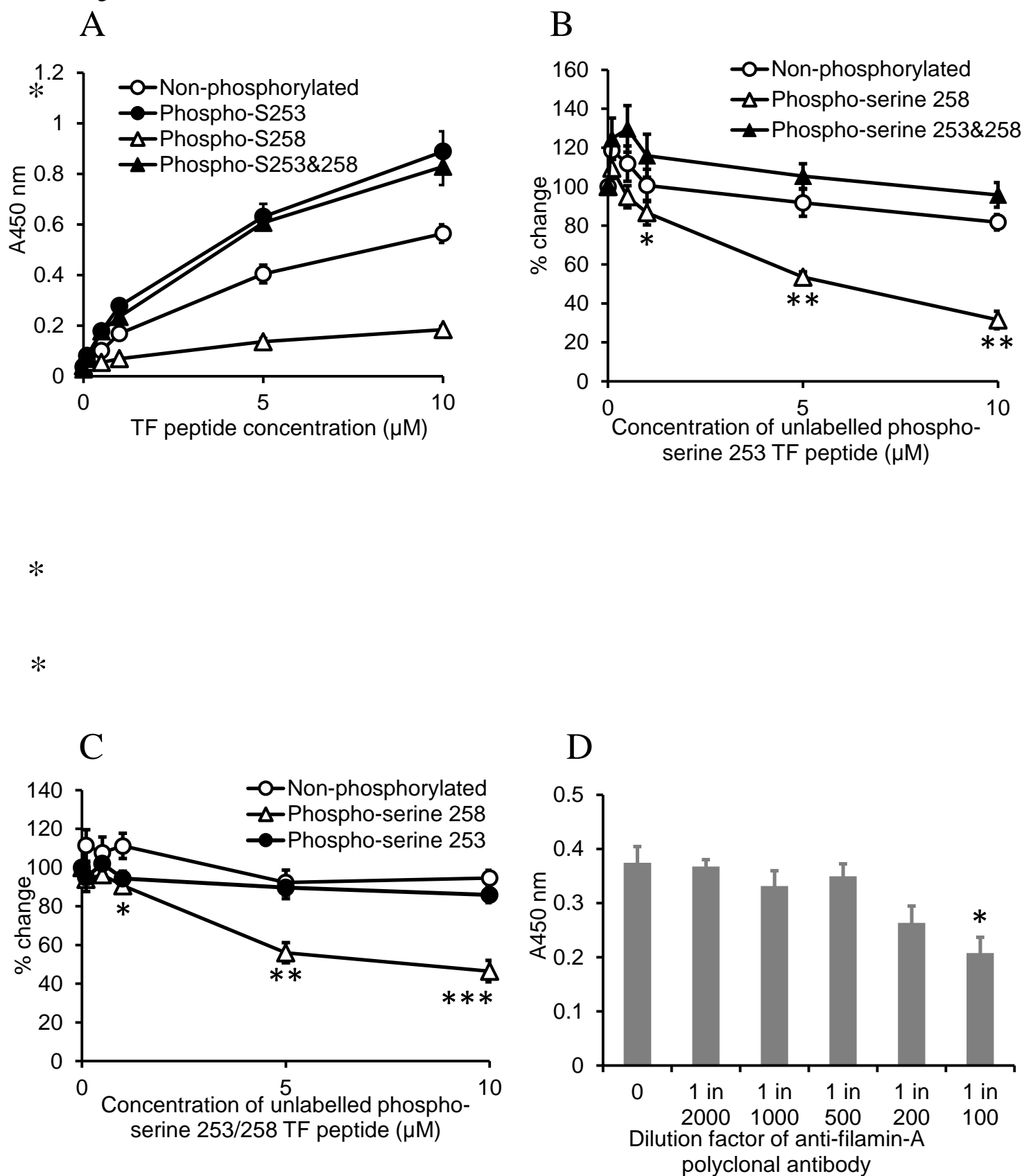


Figure 2.

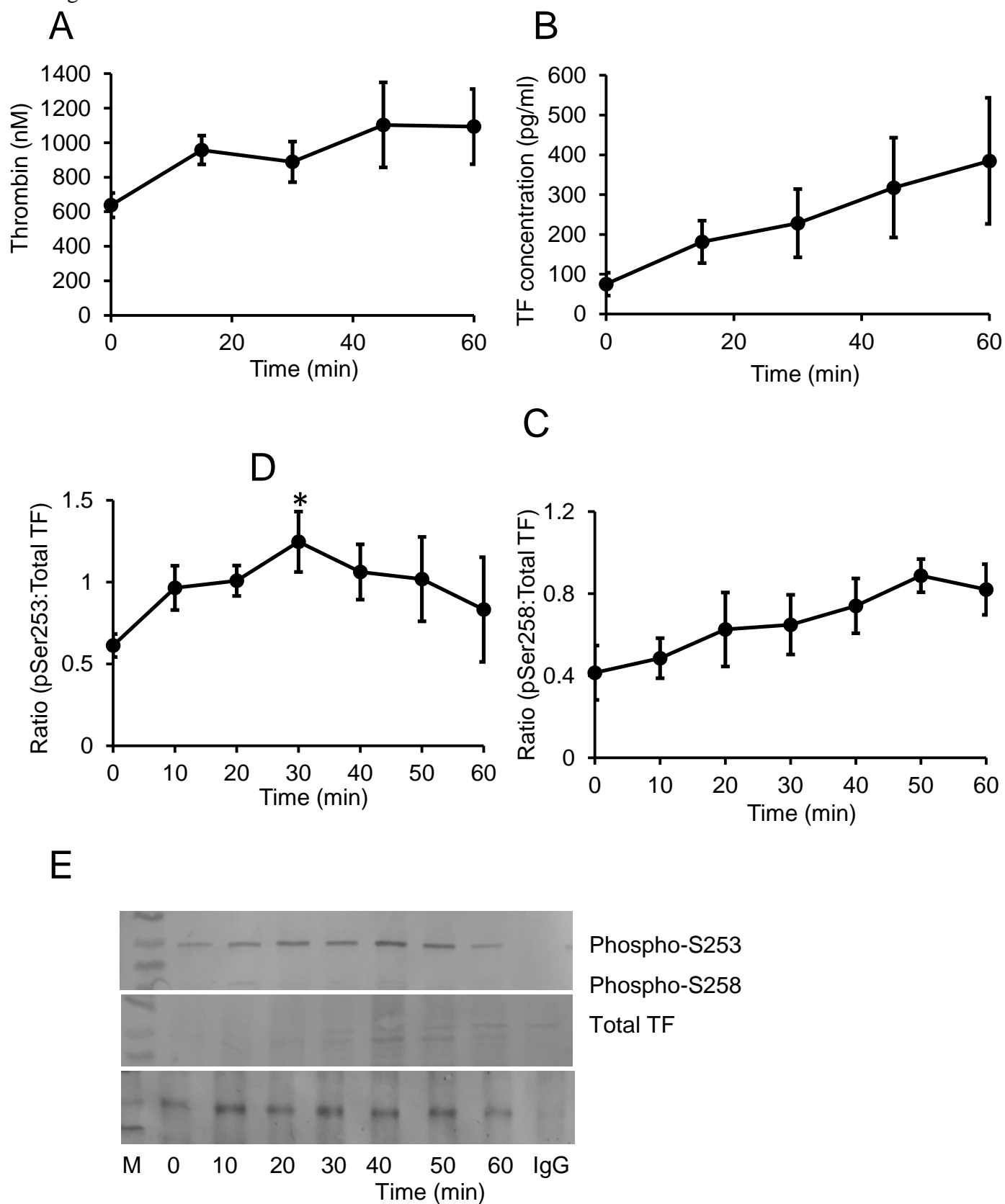


Figure 3.

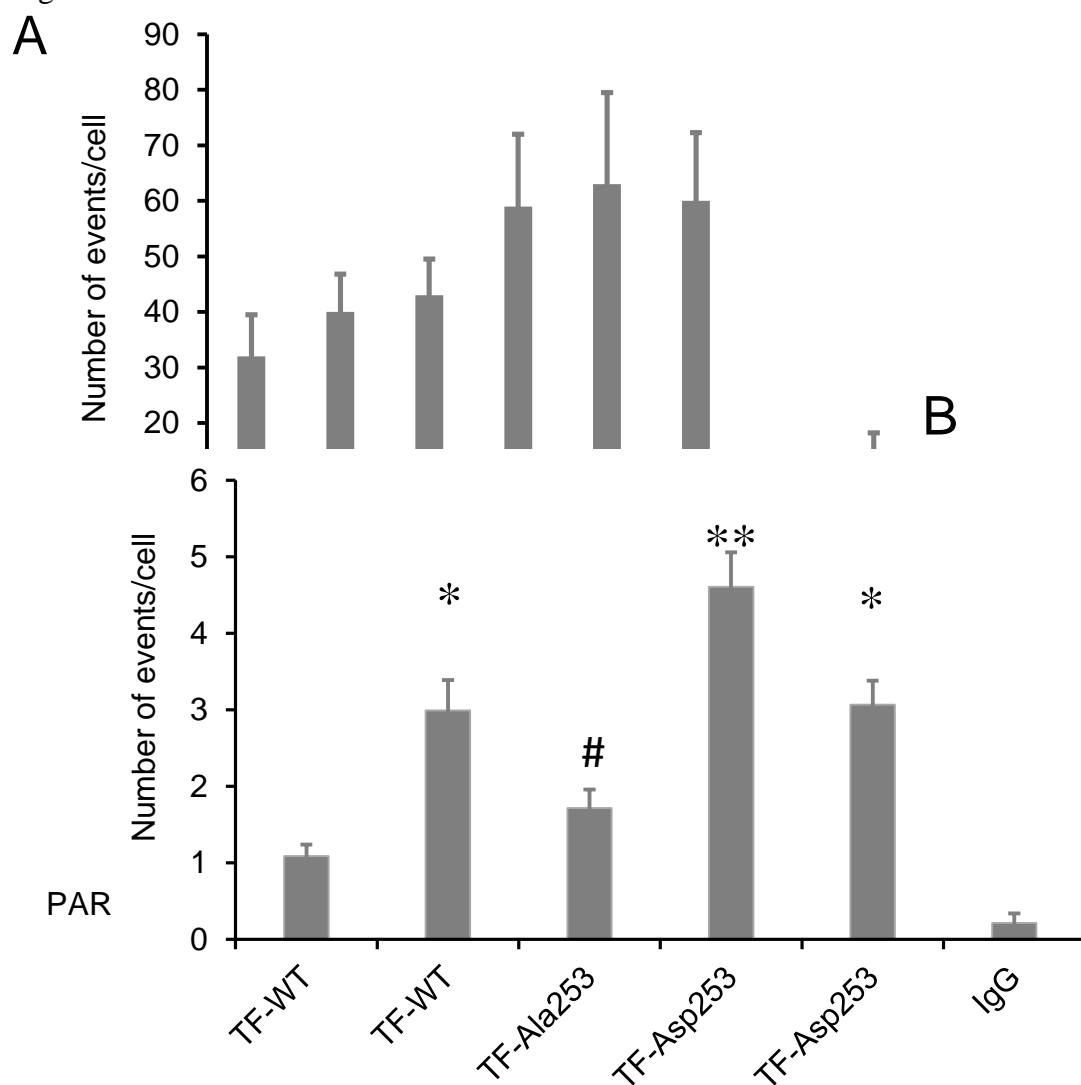


Figure 4.

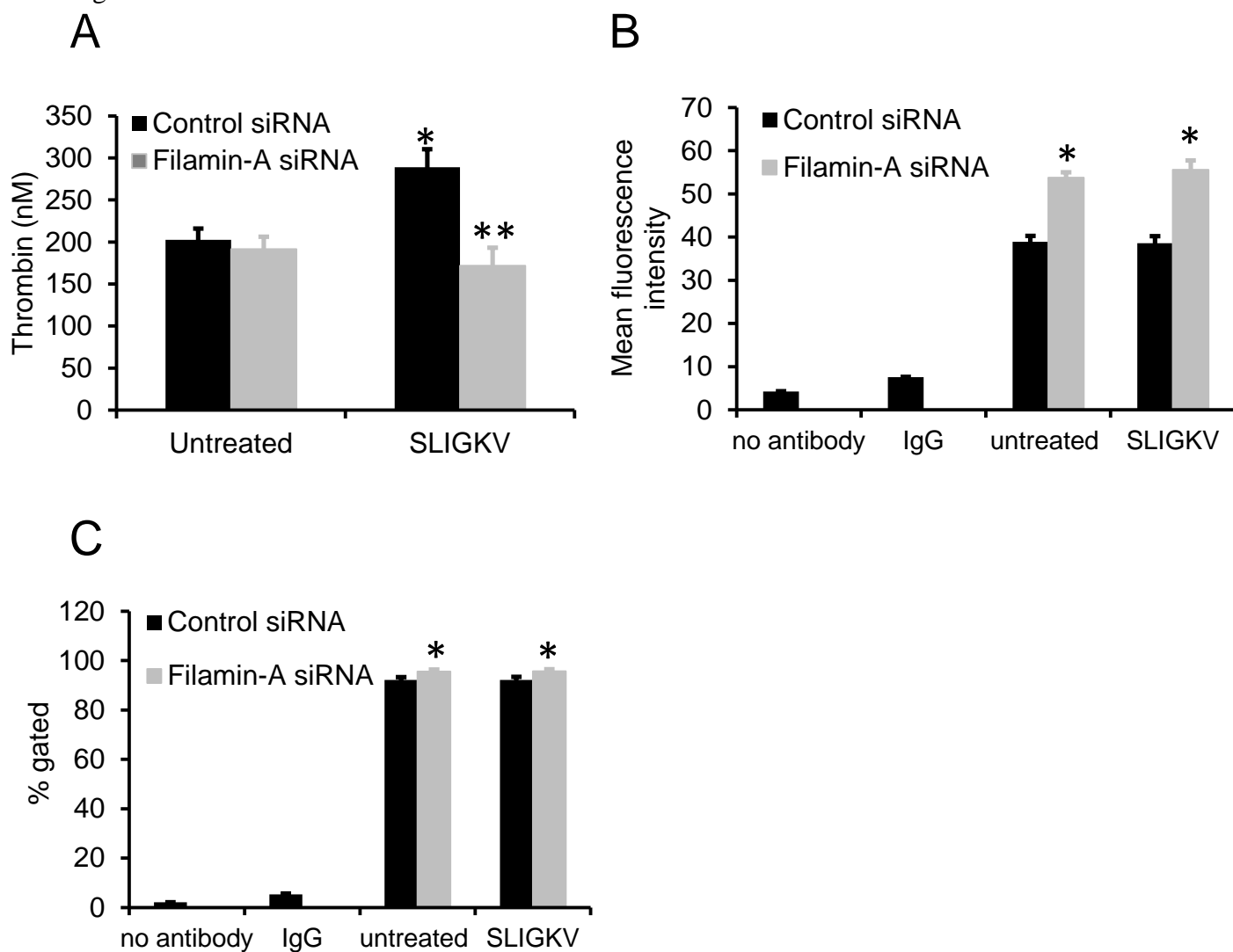


Figure 5.

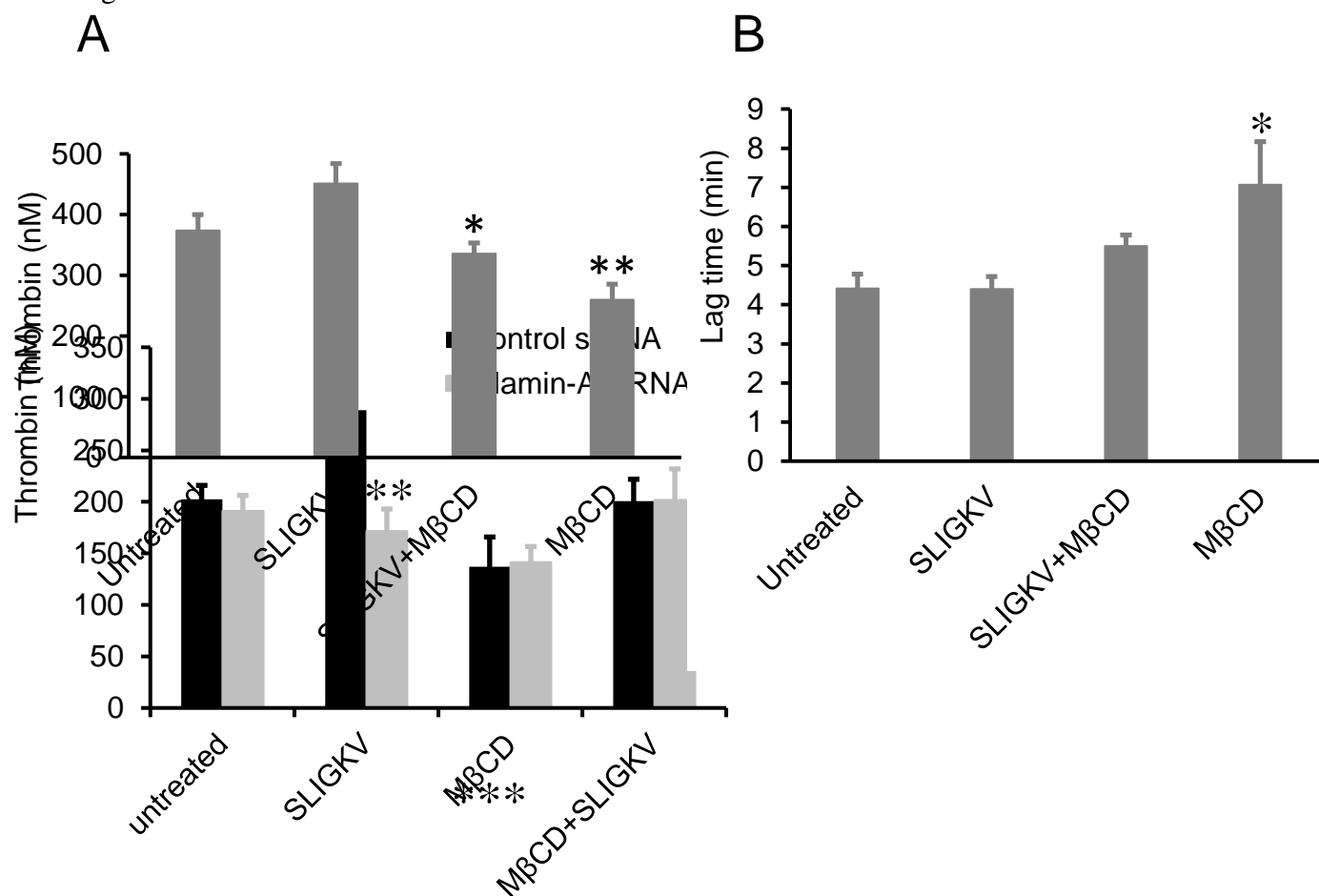


Figure 6.

